



Published in final edited form as:

Immunohorizons. ; 5(4): 157–169. doi:10.4049/immunohorizons.2100009.

Correlation of Regulatory T Cell Numbers with Disease Tolerance upon Virus Infection

Jessica B. Graham^{*}, Jessica L. Swarts^{*}, Kristina R. Edwards^{*}, Kathleen M. Voss[†], Richard Green[†], Sophia Jeng^{‡,§}, Darla R. Miller[¶], Michael A. Mooney^{‡,§}, Shannon K. McWeeney^{‡,§,||}, Martin T. Ferris[¶], Fernando Pardo-Manuel de Villena^{¶,#}, Michael Gale Jr.[‡], Jennifer M. Lund^{*,**}

^{*}Vaccine and Infectious Disease Division, Fred Hutchinson Cancer Research Center, Seattle, WA

[†]Center for Innate Immunity and Immune Disease, Department of Immunology, University of Washington School of Medicine, Seattle, WA

[‡]Division of Bioinformatics and Computational Biology, Department of Medical Informatics and Clinical Epidemiology, Oregon Health & Science University, Portland, OR

[§]OHSU Knight Cancer Institute, Oregon Health & Science University, Portland, OR

[¶]Department of Genetics, University of North Carolina at Chapel Hill, Chapel Hill, NC

^{||}Oregon Clinical and Translational Research Institute, Oregon Health & Science University, Portland, OR

[#]Lineberger Comprehensive Cancer Center, University of North Carolina at Chapel Hill, Chapel Hill, NC

^{**}Department of Global Health, University of Washington, Seattle, WA

Abstract

The goal of a successful immune response is to clear the pathogen while sparing host tissues from damage associated with pathogen replication and active immunity. Regulatory T cells (Treg) have been implicated in maintaining this balance as they contribute both to the organization of immune responses as well as restriction of inflammation and immune activation to limit immunopathology. To determine if Treg abundance prior to pathogen encounter can be used to predict the success of an antiviral immune response, we used genetically diverse mice from the collaborative cross infected with West Nile virus (WNV). We identified collaborative cross lines with extreme Treg abundance at steady state, either high or low, and used mice with these extreme phenotypes to demonstrate that baseline Treg quantity predicted the magnitude of the CD8 T cell response to

This article is distributed under the terms of the [CC BY-NC-ND Unported license](https://creativecommons.org/licenses/by-nc-nd/4.0/).

Address correspondence and reprint requests to: Dr. Jennifer M. Lund, Fred Hutchinson Cancer Research Center, 1100 Fairview Avenue N, E5-110, Seattle, WA 98109. jlund@fredhutch.org.

D.R.M., S.K.M., M.T.F., F.P.-M.d.V., M.G., and J.M.L. designed the research studies; J.B.G., J.L.S., and K.M.V. conducted experiments and acquired and analyzed data; K.R.E. and R.G. analyzed data; S.J. and M.A.M. performed data cleaning and integration; and J.B.G. and J.M.L. wrote the first draft of the manuscript. All authors read the manuscript and contributed editorial suggestions.

DISCLOSURES

The authors have no financial conflicts of interest.

WNV infection, although higher numbers of baseline Tregs were associated with reduced CD8 T cell functionality in terms of TNF and granzyme B expression. Finally, we found that abundance of CD44⁺ Tregs in the spleen at steady state was correlated with an increased early viral load within the spleen without an association with clinical disease. Thus, we propose that Tregs participate in disease tolerance in the context of WNV infection by tuning an appropriately focused and balanced immune response to control the virus while at the same time minimizing immunopathology and clinical disease. We hypothesize that Tregs limit the antiviral CD8 T cell function to curb immunopathology at the expense of early viral control as an overall host survival strategy.

INTRODUCTION

West Nile virus (WNV), a single-stranded, positive-sense RNA virus, represents an emerging pathogen in the flavivirus genus that can cause a range of clinical outcomes, including asymptomatic infection and severe disease. WNV often leads to a febrile illness and can become neuroinvasive, resulting in encephalitis, meningitis, and acute flaccid paralysis (1). Milder cases might result in chronic illness, which can manifest as long-term functional and cognitive problems (2). Although endemic to Africa and the Middle East, WNV has spread to the Western hemisphere, where it has since caused sporadic yet intense outbreaks (3).

It has previously been demonstrated that an increased frequency of peripheral regulatory T cells (Tregs) detected after WNV infection correlates with protection against severe disease in both humans and mice (4). In a retrospective study using WNV⁺ samples screened from blood donations, WNV-symptomatic individuals were found to exhibit lower Treg frequencies than asymptomatic individuals. Because these samples were identified through routine screening of WNV in blood donations, preinfection samples were not available, so it was not possible to determine if the differences in Treg frequency in asymptomatic versus symptomatic infection were solely because of infection or if they also existed at baseline. To address this, next, the frequency of Tregs in C57BL/6 mice and their disease outcome phenotypes were examined. In this inbred mouse strain, Treg frequency at baseline is consistent between mice, and the group observed that lower Treg frequencies were later observed in the blood at day 14 postinfection in mice that would ultimately succumb to WNV infection, corresponding to the finding of fewer Tregs in symptomatic humans. Although this study suggests that elevated numbers of peripheral Tregs postinfection protects against severe WNV disease in both mice and humans, it is still unclear whether Treg abundance prior to infection could predict clinical outcomes postinfection and thus serve as a predictive biomarker.

Foxp3⁺ Tregs promote tolerance and limit autoimmunity (5–7), and altered Treg function is implicated in several autoimmune conditions, including inflammatory bowel disease, rheumatoid arthritis, and multiple sclerosis (8). In the full absence of Tregs, such as in Treg-deficient scurfy mice or individuals carrying nonfunctional *Foxp3*, life-threatening multiorgan autoimmunity develops early in life (9, 10), underscoring the critical functions of Tregs in modulating immunosuppression. In the context of several infections such as HSV-1

or *Leishmania*, Tregs limit immunity that could lead to excessive collateral tissue damage (5, 11–15). In the context of other infections such as HSV-2, lymphocytic choriomeningitis virus, or RSV, Treg ablation prior to infection results in delayed pathogen clearance, suggesting that the presence of Tregs can be beneficial in facilitating and tuning an appropriately protective immune response (16–19). Using the Foxp3^{DTR} model of transient Treg ablation, we previously demonstrated that in the context of WNV infection, Tregs limit the infection-driven cytokine response from T cells during the effector phase while, at the same time, allowing for the establishment of a robust memory T cell response in the brain (20). This study, however, was performed in C57BL/6 mice, and so we were not able to assess how Tregs contribute to the range of clinical outcomes upon infection as this inbred mouse strain has a consistent disease response upon WNV infection.

Host genetics have long been recognized as an important determinant in clinical outcomes of infectious disease (21). Mouse models are commonly used to study and model immune responses to invading pathogens, yet most commonly used inbred mouse strains lack genetic diversity and can fail to recapitulate the full spectrum of symptom severities seen during infection of a human population. The use of the collaborative cross (CC) at least in part addresses these concerns. The CC is a multiparental mouse reference population that allows for the study of immune response to infection in a genetically diverse population (22). To generate the CC, a funnel breeding pattern was used to incorporate all eight founder strains, followed by inbreeding for a minimum of 20 generations (23). The resulting genetic diversity is evenly distributed across the genome and accounts for the vast majority of the variation observed in *Mus musculus* strains used in laboratory research (23). Thus, the CC model can be used to investigate the effects of genetic diversity not found in studies using single traditional inbred laboratory strains while also allowing for genotypic reproducibility because of extensive backcrossing. In this study, we use recombinant intercross CC mice (CC-RIX), which are F1 progeny from recombinant inbred CC strains. We designed the CC-RIX mouse crosses to result in lines that are heterozygous for H-2b^b, thereby allowing for the use of tetramer staining to identify WNV-specific CD8 T cells. Our group and others have previously used CC-RIX mice to study the range of phenotypes postinfection seen in humans for a variety of pathogens, including Ebola virus, influenza virus, Zika virus, SARS-CoV, *Aspergillus fumigatus*, and WNV (24–33).

Thus, to determine if Treg measures prior to pathogen encounter can be used to predict the success of an antiviral immune response, we used a screen of genetically diverse mice from the CC infected with WNV in combination with pre- and postinfection immunophenotyping and assessment of viral and disease burden. Our correlative studies use natural variation in the abundance of Tregs at baseline inherent in genetically diverse mice to demonstrate that the number of Tregs at steady state predict immune and clinical features following infection. This is consistent with our hypothesis that Tregs assist in tuning an appropriately focused and balanced immune response upon infection that serves to keep immune activation in check to limit immunopathology while, at the same time, promoting expansion of the antiviral T cell response to curb pathogen replication.

MATERIALS AND METHODS

Mice

Inbred CC mice were obtained from the Systems Genetics Core Facility at the University of North Carolina Chapel Hill (UNC), and CC-RIX were bred from these animals at UNC under an approved Institutional Animal Care and Use Committee protocol in the F.P.-M.d.V. laboratory (34). The 6–8-wk-old F1 hybrid male mice were transferred from UNC to the University of Washington (UW) and housed directly in a biosafety level 2⁺ laboratory within a specific pathogen-free barrier facility. Male 8–10-wk-old mice were used for all experiments, with 3–6 mice per experimental group. All animal experiments were approved by the UW Institutional Animal Care and Use Committee. The Office of Laboratory Animal Welfare of National Institutes of Health approved UNC (no. A3410-01) and the UW (no. A3464-01), and this study was carried out in strict compliance with the Public Health Service Policy on Humane Care and Use of Laboratory Animals.

Virus and infection

WNV TX-2002-HC (WN-TX) was propagated as previously described (35). Mice were s.c. inoculated in the rear footpad with 100 PFU WNV TX-2002-HC. Mice were monitored daily for morbidity (percentage of initial weight loss) and clinical disease scores (29).

RNA extraction and analysis

Spleen and brain were removed from mice after perfusion, RNA was extracted, and cDNA was synthesized as previously described (36). WNV expression was detected by SYBR Green quantitative RT-PCR based on the 2⁻CT method and normalized for the individual GAPDH values in each sample (31). The values represent fold expression over mock. For WNV, the values represent the fold increase in signal over an arbitrarily low value in the mock that represents a virus-null sample.

Flow cytometry

Following euthanasia, mice were perfused with 10ml PBS to remove any residual intravascular leukocytes, and spleens and brains were prepared for flow cytometry staining as previously described using the Abs listed in Table I (29–33). All Abs were tested using cells from the eight CC founder strains to confirm that Ab clones were compatible with the CC mice prior to being used for testing. We used CD4, Foxp3, CCR5, CD25, CD44, CD73, CTLA-4, CXCR3, GITR, and ICOS in our Treg panel. In the T cell panel, we used CD3, CD4, CD8, CCR5, CD25, CD44, CXCR3, ICOS, WNV tetramer (NS4b epitope), and Ki67. We used CD3, CD4, CD8, IFN- γ , and TNF in our intracellular cytokine staining panel, along with anti-CD3/CD28 polyclonal stimulation or NS4b peptide stimulation. Gating schemes were used as reported previously (30). Tetramer-positive, WNV-specific (NS4b epitope) T cells were identified after gating on CD8⁺ cells. All flow cytometry data were acquired on a BD LSR II and analyzed with FlowJo software.

Statistical analysis

Statistical analyses were performed using GraphPad Prism. When comparing groups, *t* tests or Mann–Whitney tests were employed. Outliers were identified using the robust regression and outlier removal method (ROUT) ($Q = 1\%$). Error bars are \pm SD.

RESULTS

Genetically diverse mice present with a range of Treg numbers in the spleen and brain at steady state

Using 103 CC-RIX lines (Table II), we conducted a comprehensive screen to identify the diversity in immune responses to WNV infection resulting from natural genetic variation. We have previously reported on the range of phenotypes that exist in the spleen at steady state (30), including variation in the frequency of T cell subsets, proportions of those T cells expressing various activation markers, and frequency of cells expressing tissue migration markers or producing inflammatory cytokines within the spleen. In this study, we first examined the average number of splenic Tregs at the baseline in each of the 103 CC-RIX lines in the screen, rank ordering the lines from the least to the greatest number of Tregs at baseline (Fig. 1A). This demonstrates a wide range (from 3×10^4 – 8×10^5) in splenic Treg numbers based on CC-RIX line, similar to the differences that we previously demonstrated for Treg frequency across these same CC-RIX (30). Next, we identified CC-RIX lines with the top 10% ($n = 10$) and bottom 10% ($n = 10$) number of splenic Tregs at baseline, shown in Table II and Fig. 1B. There was a more than 10-fold difference in the number of baseline Tregs in the top 10% group compared with the bottom 10% group, thereby validating this extreme phenotype approach and demonstrating that the CC is a novel resource to study the effect of various baseline numbers of baseline Tregs on the course of disease and immunity upon subsequent infection.

Higher Treg numbers at baseline correlate with an activated Treg phenotype postinfection

After identifying differences in preinfection Treg abundance at steady state, we next wanted to further characterize the Treg number and phenotype over the course of WNV infection both in the spleen and in a peripheral viral target tissue, the brain.

Although Treg numbers do increase postinfection in the Treg-low group in both spleen and brain, the number of Tregs in the Treg-low group remain below the Treg-high group over the time course of infection in both spleen and brain and in fact do not expand over the course of infection (Fig. 1C). Furthermore, at baseline in the spleen, the Treg-high group has increased numbers of Tregs that are CCR5, CD25, CD44, CD73, CTLA-4, CXCR3, GITR, or ICOS-positive compared with the Treg-low group. These numbers of activated Tregs persist over the time course of infection in the spleen (Fig. 2A). Splenic Treg numbers at baseline also predicts Treg phenotype postinfection in the brain, with the Treg-high group also maintaining increased numbers of activated Tregs over the time course of infection (Fig. 2B). These differences in the brain Treg numbers are particularly strong at both 21 and 28 d postinfection. Collectively, baseline splenic Treg numbers correlated with Treg abundance and phenotype after infection in both lymphoid tissue and the brain following infection with WNV.

Baseline Treg numbers correlate with the T cell phenotype in lymphoid and peripheral tissues at steady state and following infection

After observing that higher Treg numbers at baseline correlated with an activated Treg phenotype postinfection, we next wanted to examine the conventional T cell phenotypes in both spleen and brain at steady state and following infection between our extreme Treg groups. As with Treg activation, higher Treg numbers at baseline correlated with an increased frequency of CD44⁺ memory phenotype CD8 T cells at baseline and 7 d postinfection in the spleen (Fig. 3A). In the brain, mice in the Treg-high group also had a significantly elevated frequency of CD8 T cells with a memory CD44⁺ phenotype at baseline, although not at day 7 (d7) postinfection (Fig. 3A). Mice in the Treg-high and Treg-low groups had similar proportions of CD4 T cells expressing CD44 in the spleen and brain both at baseline as well as d7 postinfection (Fig. 3B). We also assessed the frequency of Ki67⁺ T cells as an indication of cells that have recently undergone proliferation and are thus likely to be active in the immune response. In both the spleen and brain, there was no significant difference in the baseline frequency of CD8 or CD4 T cells expressing Ki67 in the Treg-high or Treg-low groups, and whereas the frequency of Ki67⁺ cells increased considerably by d7 postinfection, the increase was largely similar between Treg-high and Treg-low groups (Fig. 3C, 3D). Notably, however, mice in the Treg-high group had significantly more CD8 T cells expressing Ki67 as compared with mice in the Treg-low group in the spleen at d7 postinfection (Fig. 3C). Finally, we also assessed the magnitude of the WNV-specific CD8 T cell response as detected by NS4b tetramer stain. Mice in the Treg-high group had a significantly higher fraction of CD8 T cells specific for this immunodominant WNV epitope at d7 postinfection in both the spleen and the brain as compared with animals in the Treg-low group (Fig. 3E), suggesting a positive association between the number of Tregs at baseline and the magnitude of the WNV-specific CD8 T cell response in different tissues following infection. Overall, the presence of elevated numbers of splenic Tregs at baseline is associated with increased numbers of activated CD8 T cells in the spleen and brain, both at steady state and postinfection.

Elevated numbers of Tregs at baseline are associated with altered CD8 T cell cytokine responses upon infection

Thus far, we have observed that mice from CC-RIX lines with elevated numbers of splenic Tregs at baseline have increased frequencies of activated Treg and CD8 T cells, including WNV-specific CD8 T cells, in both the spleen and brain following infection. Therefore, we next wanted to examine the CD8 T cell cytokine response postinfection to characterize not only the magnitude of the CD8 T cell response but also the quality of effector function. Thus, total lymphocytes from either spleen or brain excised d7 postinfection were stimulated with WNV NS4b peptide or anti-CD3/CD28 to assess the WNV-specific or polyclonally induced cytokine response, respectively. Unsurprisingly, the magnitude of the CD8 T cell cytokine response was stronger with polyclonal stimulation than NS4b peptide (Fig. 4). There was no difference in the proportion of CD8 T cells in the spleen that expressed IFN γ in response to either viral or polyclonal stimulus (Fig. 4A, 4B). In mice from the Treg-low group, we observed a significant increase in the proportion of CD8 T cells from the spleen that expressed TNF following stimulation with NS4b peptide (Fig. 4A), demonstrating that lower numbers of Tregs at baseline are associated with an elevated TNF response driven by

virus postinfection, although there was no difference following polyclonal stimulation (Fig. 4B). Similarly, in the brain, mice from the Treg-low group had a significant increase in the frequency of CD8 T cells that expressed TNF following polyclonal stimulation, although not with NS4b peptide (Fig. 4C, 4D). Uniquely, in the brain, mice from the Treg-high group had a significantly increased fraction of CD8 T cells that expressed IFN γ in response to NS4b peptide stimulation as compared with the Treg-low group (Fig. 4C). Overall, our data demonstrate that mice with a lower baseline number of splenic Tregs have elevated frequencies of TNF-expressing CD8 T cells in the spleen and brain after WNV infection, thereby demonstrating that steady-state Treg abundance assists in tuning the antipathogen CD8 T cell functional capacity.

Elevated baseline Treg numbers predict elevated viral loads following WNV infection

After identifying extreme phenotype Treg-high and Treg-low cohorts that associate with differing CD8 T cell outcomes upon infection, we next wanted to examine how the baseline Treg number correlates with postinfection clinical score and disease measurements as well as viral titers. Plotting the WNV loads, detected by PCR, against the number of splenic Tregs at baseline, we found that increased numbers of Tregs preinfection correlated with a higher viral load (VL) at days 4 and 7 postinfection, but there was no significant correlation between Treg number and West Nile VL at d2 or day 12 postinfection (Fig. 5A). Furthermore, there was no association between the number of splenic Tregs at baseline and the brain VL at d7 or day 12 postinfection (Fig. 5B). When we assessed average weight loss at day 10 (d10) postinfection, we found a significant correlation with increased numbers of splenic Tregs at baseline and increased weight loss following infection (Fig. 5C). However, there was no association between baseline splenic Treg number and maximum clinical score or mortality following WNV infection (Fig. 5C). Taken together, preinfection Treg abundance predicts higher splenic VL at days 4 and 7 postinfection as well as increased clinical disease as indicated by weight loss but not clinical score. Previously, it has been observed that elevated postinfection Treg frequency was associated with enhanced survival from WNV in C57BL/6 mice (4), although we note that use of inbred mice in that study precluded an assessment of how steady-state variability in Treg numbers impacts viral kinetics and disease progression upon WNV infection as there is essentially no variability in Treg abundance within individual mice of C56BL/6 background compared with variability between CC-RIX lines (Fig. 1A). Finally, we also assessed the relationship between spleen or brain VL and disease progression by plotting average VL against average weight loss at d10 postinfection for all of the CC-RIX lines examined. Notably, although spleen VL at day 2 (d2) postinfection was not correlated with weight loss, spleen VL at day 4 and d7 postinfection, as well as brain VL at d7 and day 12 postinfection, was positively correlated with weight loss postinfection (Fig. 5D). Thus, it appears that elevated VL later in the time course of infection are associated with a higher burden of disease but that the very earliest VL in the spleen can be tolerated without necessarily leading to clinical disease.

Lower baseline number of Tregs is associated with a subsequent cytotoxic phenotype of WNV-specific CD8 T cells upon infection

Given our finding that a higher number of baseline splenic Tregs is associated with increased splenic VL at days 4 and 7 postinfection (Fig. 5A), we reasoned that this heightened level of

Treg-mediated immunosuppression could additionally dampen the antiviral immune response in ways beyond cytokine production (Fig. 4). Thus, we performed a smaller-scale validation study in which we tested five CC-RIX lines with high ($n = 2$) or low ($n = 3$) numbers of splenic Tregs at baseline (Fig. 6A) for an additional CD8 T cell functional marker that was not included in the original screen: granzyme B expression. This additional immunophenotyping study revealed that having a higher baseline number of splenic Tregs was associated with a reduced cytotoxic phenotype of WNV-specific CD8 T cells 7 d postinfection (Fig. 6B). Additionally, higher numbers of splenic Tregs prior to infection was associated with a statistical trend toward reduced numbers of bulk CD8 T cells in the spleen that expresses granzyme B (Fig. 6C). Thus, our data suggest that elevated numbers of Treg preinfection may lead to an inhibitory tuning of the antiviral immune response toward a reduced capacity of splenic CD8 T cells to express TNF (Fig. 4A) plus a reduced cytotoxic CD8 T cell response, both Ag specific as well as overall.

Homeostatic Treg phenotype and abundance contributes to disease tolerance upon infection with WNV

Given our finding that a larger Treg population at steady state is associated both with a reduction in CD8 T cell production of TNF (Fig. 4) as well as granzyme B (Fig. 6), yet also with enhanced VL at d7 postinfection (Fig. 5A, 5B), we hypothesized that Tregs balance the immune response to WNV to best spare the host from disease if not virus replication. We demonstrated that the very early VL in the spleen did not predict disease in terms of weight loss (Fig. 5D), and so we hypothesized that Tregs tune the immune response to avoid excess immunopathology, even at the expense of early viral clearance. This concept, which has been termed “disease tolerance,” has previously been discussed as a possible mechanism whereby the host tolerates some degree of infectious burden to limit immunopathology as an overall survival strategy (37). Thus, we wanted to further investigate how Tregs may play a role in disease tolerance during WNV infection. To this end, we identified CC-RIX lines with extreme phenotypes (Fig. 7A): 1) lines that had a high splenic VL at d2 postinfection but had little to no evidence of disease throughout the course of infection (VL-no disease; $n = 6$ lines) or 2) lines that had low splenic VL at d2 postinfection and beyond but did have evidence of disease in terms of mortality and/or mean weight loss $> 10\%$ (disease low VL; $n = 6$ lines). When we examined the preinfection baseline number of Tregs in these two groups, we found that there was no difference in the overall number of Tregs (Fig. 7B). However, when we assessed the number of Tregs expressing select phenotypic markers, we found that there was a statistically significant increase in the number of CD44⁺ Treg and CD25⁺ Treg in the spleen at baseline in mice from CC-RIX lines in the VL-no disease group that had high splenic VL at d2 postinfection without developing disease throughout the course of WNV infection (Fig. 7B). Finally, we also examined the relationship between the number of splenic CD44⁺ Tregs at baseline in all of the CC-RIX lines examined and the d2 splenic VL and found a positive correlation, yet with no association between CD44⁺ Tregs and weight loss, clinical score, or mortality (Fig. 7C). Altogether, this suggests that CD44⁺ Tregs may play a role in mediating disease tolerance by tuning the immune response to tolerate higher early VL, at least in part by reducing the functional potential of CD8 T cells so as to spare the host excessive clinical disease.

DISCUSSION

A hallmark of a so-called successful immune response results in clearance of the pathogen while at the same time sparing host tissues from damage associated with pathogen replication and active immunity. This balance is exceptionally critical to achieve in the context of neuroinvasive WNV infection as the virus is ideally cleared prior to neuroinvasion or, barring that, cleared from the CNS without resulting in injury to nonregenerating neurons. Our previous studies demonstrated that Tregs play a role in balancing immunity to virus infection and WNV in particular (4, 17, 19, 20, 31, 32), so in this study, we used data from a screen of genetically diverse mice from the CC to evaluate how baseline Treg abundance contributes both to organization of the antipathogen immune responses as well as to restricting inflammation and immune activation to limit immunopathology. Importantly, use of the CC allows for an assessment of diversity in Treg numbers rather than complete ablation of the population and so better reflects the diversity in this subset reported in humans. Consistent with our previous studies, at steady state, we observed a range of Treg abundance in the spleen in mice from different CC-RIX lines [Fig. 1 and (30)], and we used this diversity to demonstrate that preinfection Treg abundance and phenotype correlated with VL upon infection, with increased numbers of Tregs preinfection correlating with a higher VL at days 4 and 7 postinfection. Previous studies were conducted using samples from the postinfection period rather than prospectively collected samples (4), and so it was unclear from that previous study if the identified association of reduced Tregs with symptomatic WNV infection was predictive of severe disease or a manifestation of severe disease. Results from our study suggest that preinfection “set point” Treg abundance and phenotype differentially affects disease severity upon infection as compared with the postinfection frequency.

The underlying reason for elevated numbers of Tregs in some CC-RIX is presumed to be at least in part because of genetic factors, although we have not yet identified quantitative trait loci associated with high or low numbers of Tregs at steady state. Thus, our findings rely largely on correlative studies at present, although future studies will aim to identify host genetic regions associated with Treg abundance at steady state. Furthermore, it is likely that genetic differences between CC-RIX lines contribute directly to diversity in other immune phenotypes in addition to Treg number, and so we acknowledge that this is a potential confounding factor in our study. Along these lines, we have found that higher numbers of baseline Tregs correlate with elevated numbers of activated CD8 T cells (Fig. 3), which raises the question of which came first; does T cell activation lead to Treg conversion or expansion, possibly through increased availability of IL-2, or perhaps host genetics controls both phenotypic traits? Regardless of the answer, it is possible that these activated T cells are not able to appropriately participate in anti-WNV immune responses as increased VL in the spleen were found to be associated with increased numbers of baseline Tregs (Fig. 5), thereby suggesting that these Tregs are restricting or tuning the antipathogen immune response. Indeed, we demonstrated that higher numbers of baseline Treg were associated with CD8 T cells with reduced functional potential in terms of TNF and granzyme B expression (Figs. 4 and 6), and it has been previously demonstrated that CD8 T cell cytotoxic function is required for clearance of WNV from the CNS of infected mice (38,

39). We found the reduced CD8 T cell expression of granzyme B association with higher baseline Treg abundance in the case of both polyclonal or WNV-specific T cells (Fig. 6B), which could be the result of altered priming of T cells in the context of higher numbers of Tregs as Tregs can outcompete with T cells for access to APCs through their high-affinity interactions with B7 molecules via CTLA-4. In addition, in the case of total CD8 T cells (Fig. 6C), it is possible that increased Treg-mediated immunosuppression leads to a reduction in inflammatory cytokine production that can then drive bystander activation of memory T cells. In both cases, this reduced cytotoxic activity may at least in part explain the increased splenic viral titers observed in mice with higher numbers of Tregs, although the mechanism whereby Tregs restrict CD8 T cell cytotoxic function in the context of WNV needs to be further investigated.

Finally, to further investigate our hypothesis that Tregs promote disease tolerance in the context of WNV infection, we identified CC-RIX lines with high early VL but no disease and lines with disease but low VL throughout the course of infection. Because of our finding that mice from lines without disease but with a high early VL had more CD44⁺ Tregs prior to infection (Fig. 6B), we hypothesized that these Tregs actively restrain immune activation to limit collateral damage and WNV disease, even at the expense of rapid viral control. This appears to be a successful host survival strategy as there is not an associated cost in terms of clinical score, weight loss, or mortality (Fig. 7C). CD44 costimulation has previously been shown to promote expression of Foxp3, in addition to increasing the production of IL-10 and TGF β expression (40), suggesting that CD44⁺ Tregs have an enhanced suppressive function. Although we predict that these abundant CD44⁺ Tregs play a role in dampening both innate immune activation, such as bystander T cell activation, and the Ag-specific adaptive immune response, further investigation is needed to identify the mechanisms whereby CD44⁺ Tregs serve to limit early immunity to promote disease tolerance. However, our study, although largely correlative in nature, points to a critical role for Tregs in achieving an appropriately focused and balanced immune response upon infection that serves to keep immune activation in check to limit immunopathology while, at the same time, promoting expansion of the antiviral T cell response to curb pathogen replication. Altogether, we propose that Tregs promote disease tolerance by tuning the immune response to curb immunopathology, at least in part by limiting antiviral CD8 T cell function. Although this occurs at the expense of early viral control, this is tolerated to provide the host with an overall host survival strategy by minimizing viral disease.

ACKNOWLEDGMENTS

We thank our collaborators in the Systems Immunogenetics Group for helpful discussions and generation of mice. In particular, we thank Ginger Shaw for generating the RIX mice used in this study.

This work was supported by National Institutes of Health grants U19AI100625 and R01AI141435.

Abbreviations used in this article:

CC	collaborative cross
CC-RIX	recombinant intercross CC mice

d2	day 2
d7	day 7
d10	day 10
ROUT	robust regression and outlier removal method
Treg	regulatory T cell
UNC	University of North Carolina Chapel Hill
UW	University of Washington
VL	viral load
WNV	West Nile virus

REFERENCES

1. Sejvar JJ 2007. The long-term outcomes of human West Nile virus infection. *Clin. Infect. Dis* 44:1617–1624. [PubMed: 17516407]
2. Murray KO, Walker C, and Gould E. 2011. The virology, epidemiology, and clinical impact of West Nile virus: a decade of advancements in research since its introduction into the Western Hemisphere. *Epidemiol. Infect* 139: 807–817. [PubMed: 21342610]
3. Hughes AL, Piontkivska H, and Foppa I. 2007. Rapid fixation of a distinctive sequence motif in the 3' noncoding region of the clade of West Nile virus invading North America. *Gene* 399:152–161. [PubMed: 17587514]
4. Lanteri MC, O'Brien KM, Purtha WE, Cameron MJ, Lund JM, Owen RE, Heitman JW, Custer B, Hirschhorn DF, Tobler LH, et al. 2009. Tregs control the development of symptomatic West Nile virus infection in humans and mice. *J. Clin. Invest* 119: 3266–3277. [PubMed: 19855131]
5. Belkaid Y, and Tarbell K. 2009. Regulatory T cells in the control of host-microorganism interactions (*). *Annu. Rev. Immunol* 27: 551–589. [PubMed: 19302048]
6. Campbell DJ, and Koch MA. 2011. Phenotypical and functional specialization of FOXP3+ regulatory T cells. *Nat. Rev. Immunol* 11: 119–130. [PubMed: 21267013]
7. Kim JM, Rasmussen JP, and Rudensky AY. 2007. Regulatory T cells prevent catastrophic autoimmunity throughout the lifespan of mice. *Nat. Immunol* 8:191–197. [PubMed: 17136045]
8. Buckner JH 2010. Mechanisms of impaired regulation by CD4(+)CD25(+)FOXP3(+) regulatory T cells in human autoimmune diseases. *Nat. Rev. Immunol* 10: 849–859. [PubMed: 21107346]
9. Gambineri E, Torgerson TR, and Ochs HD. 2003. Immune dysregulation, polyendocrinopathy, enteropathy, and X-linked inheritance (IPEX), a syndrome of systemic autoimmunity caused by mutations of FOXP3, a critical regulator of T-cell homeostasis. *Curr. Opin. Rheumatol* 15: 430–435. [PubMed: 12819471]
10. Brunkow ME, Jeffery EW, Hjerrild KA, Paepers B, Clark LB, Yasayko SA, Wilkinson JE, Galas D, Ziegler SF, and Ramsdell F. 2001. Disruption of a new forkhead/winged-helix protein, scurf, results in the fatal lymphoproliferative disorder of the scurfy mouse. *Nat. Genet* 27: 68–73. [PubMed: 11138001]
11. Belkaid Y, Piccirillo CA, Mendez S, Shevach EM, and Sacks DL. 2002. CD4+CD25+ regulatory T cells control *Leishmania major* persistence and immunity. *Nature* 420: 502–507. [PubMed: 12466842]
12. Belkaid Y, and Rouse BT. 2005. Natural regulatory T cells in infectious disease. *Nat. Immunol* 6: 353–360. [PubMed: 15785761]
13. Sarangi PP, Sehrawat S, Suvas S, and Rouse BT. 2008. IL-10 and natural regulatory T cells: two independent anti-inflammatory mechanisms in herpes simplex virus-induced ocular immunopathology. *J. Immunol* 180: 6297–6306. [PubMed: 18424753]

14. Sehrawat S, Suvas S, Sarangi PP, Suryawanshi A, and Rouse BT. 2008. In vitro-generated antigen-specific CD4⁺ CD25⁺ Foxp3⁺ regulatory T cells control the severity of herpes simplex virus-induced ocular immunoinflammatory lesions. *J. Virol* 82: 6838–6851. [PubMed: 18480441]
15. Suvas S, Azkur AK, Kim BS, Kumaraguru U, and Rouse BT. 2004. CD4⁺CD25⁺ regulatory T cells control the severity of viral immunoinflammatory lesions. *J. Immunol* 172: 4123–4132. [PubMed: 15034024]
16. Fulton RB, Meyerholz DK, and Varga SM. 2010. Foxp3⁺ CD4 regulatory T cells limit pulmonary immunopathology by modulating the CD8 T cell response during respiratory syncytial virus infection. *J. Immunol* 185: 2382–2392. [PubMed: 20639494]
17. Lund JM, Hsing L, Pham TT, and Rudensky AY. 2008. Coordination of early protective immunity to viral infection by regulatory T cells. *Science* 320: 1220–1224. [PubMed: 18436744]
18. Ruckwardt TJ, Bonaparte KL, Nason MC, and Graham BS. 2009. Regulatory T cells promote early influx of CD8⁺ T cells in the lungs of respiratory syncytial virus-infected mice and diminish immunodominance disparities. *J. Virol* 83: 3019–3028. [PubMed: 19153229]
19. Soerens AG, Da Costa A, and Lund JM. 2016. Regulatory T-cells are essential to promote proper CD4 T-cell priming upon mucosal infection. *Mucosal Immunol.* 9: 1395–1406. [PubMed: 27007674]
20. Graham JB, Da Costa A, and Lund JM. 2014. Regulatory T cells shape the resident memory T cell response to virus infection in the tissues. *J. Immunol* 192: 683–690. [PubMed: 24337378]
21. Hill AV 2001. The genomics and genetics of human infectious disease susceptibility. *Annu. Rev. Genomics Hum. Genet* 2: 373–400. [PubMed: 11701655]
22. Threadgill DW, Miller DR, Churchill GA, and de Villena FP. 2011. The collaborative cross: a recombinant inbred mouse population for the systems genetic era. *ILAR J.* 52: 24–31. [PubMed: 21411855]
23. Threadgill DW, and Churchill GA. 2012. Ten years of the collaborative cross. *Genetics* 190: 291–294. [PubMed: 22345604]
24. Rasmussen AL, Okumura A, Ferris MT, Green R, Feldmann F, Kelly SM, Scott DP, Safronetz D, Haddock E, LaCasse R, et al. 2014. Host genetic diversity enables Ebola hemorrhagic fever pathogenesis and resistance. *Science* 346: 987–991. [PubMed: 25359852]
25. Ferris MT, Aylor DL, Bottomly D, Whitmore AC, Aicher LD, Bell TA, Bradel-Tretheway B, Bryan JT, Buus RJ, Gralinski LE, et al. 2013. Modeling host genetic regulation of influenza pathogenesis in the collaborative cross. *PLoS Pathog.* 9: e1003196. [PubMed: 23468633]
26. Manet C, Simon-Lorière E, Jouvion G, Hardy D, Prot M, Conquet L, Flamand M, Panthier J-J, Sakuntabhai A, and Montagutelli X. 2020. Genetic diversity of collaborative cross mice controls viral replication, clinical severity, and brain pathology induced by Zika virus infection, independently of *Oas1b*. *J. Virol* 94: e01034–19. [PubMed: 31694939]
27. Gralinski LE, Ferris MT, Aylor DL, Whitmore AC, Green R, Frieman MB, Deming D, Menachery VD, Miller DR, Buus RJ, et al. 2015. Genome wide identification of SARS-CoV susceptibility loci using the collaborative cross. *PLoS Genet.* 11: e1005504. [PubMed: 26452100]
28. Durrant C, Tayem H, Yalcin B, Cleak J, Goodstadt L, de Villena FP, Mott R, and Iraqi FA. 2011. Collaborative cross mice and their power to map host susceptibility to *Aspergillus fumigatus* infection. *Genome Res.* 21: 1239–1248. [PubMed: 21493779]
29. Graham JB, Swarts JL, and Lund JM. 2017. A mouse model of West Nile virus infection. *Curr. Protoc. Mouse Biol* 7: 221–235. [PubMed: 29261232]
30. Graham JB, Swarts JL, Mooney M, Choonoo G, Jeng S, Miller DR, Ferris MT, McWeeney S, and Lund JM. 2017. Extensive homeostatic T cell phenotypic variation within the collaborative cross. *Cell Rep.* 21: 2313–2325. [PubMed: 29166619]
31. Graham JB, Swarts JL, Thomas S, Voss KM, Sekine A, Green R, Ireton RC, Gale M, and Lund JM. 2019. Immune correlates of protection from West Nile virus neuroinvasion and disease. *J. Infect. Dis* 219: 1162–1171. [PubMed: 30371803]
32. Graham JB, Swarts JL, Wilkins C, Thomas S, Green R, Sekine A, Voss KM, Ireton RC, Mooney M, Choonoo G, et al. 2016. A mouse model of chronic West Nile virus disease. *PLoS Pathog.* 12: e1005996. [PubMed: 27806117]

33. Graham JB, Thomas S, Swarts J, McMillan AA, Ferris MT, Suthar MS, Treuting PM, Ireton R, Gale M Jr., and Lund JM. 2015. Genetic diversity in the collaborative cross model recapitulates human West Nile virus disease outcomes. *mBio* 6: e00493–15. [PubMed: 25944860]
34. Welsh CE, Miller DR, Manly KF, Wang J, McMillan L, Morahan G, Mott R, Iraqi FA, Threadgill DW, and de Villena FP-M. 2012. Status and access to the collaborative cross population. [Published erratum appears in 2014 *Mamm Genome*. 25: 192.] *Mamm. Genome* 23: 706–712. [PubMed: 22847377]
35. Suthar MS, Ma DY, Thomas S, Lund JM, Zhang N, Daffis S, Rudensky AY, Bevan MJ, Clark EA, Kaja MK, et al. 2010. IPS-1 is essential for the control of West Nile virus infection and immunity. *PLoS Pathog.* 6: e1000757. [PubMed: 20140199]
36. Green R, Wilkins C, Thomas S, Sekine A, Hendrick DM, Voss K, Ireton RC, Mooney M, Go JT, Choonoo G, et al. 2017. Oas1b-dependent immune transcriptional profiles of West Nile virus infection in the collaborative cross. *G3 (Bethesda)* 7: 1665–1682. [PubMed: 28592649]
37. Medzhitov R, Schneider DS, and Soares MP. 2012. Disease tolerance as a defense strategy. *Science* 335: 936–941. [PubMed: 22363001]
38. Shrestha B, Samuel MA, and Diamond MS. 2006. CD8+ T cells require perforin to clear West Nile virus from infected neurons. *J. Virol* 80: 119–129. [PubMed: 16352536]
39. Wang Y, Lobigs M, Lee E, and Müllbacher A. 2004. Exocytosis and Fas mediated cytolytic mechanisms exert protection from West Nile virus induced encephalitis in mice. *Immunol. Cell Biol* 82: 170–173. [PubMed: 15061770]
40. Bollyky PL, Falk BA, Long SA, Preisinger A, Braun KR, Wu RP, Evanko SP, Buckner JH, Wight TN, and Nepom GT. 2009. CD44 costimulation promotes FoxP3+ regulatory T cell persistence and function via production of IL-2, IL-10, and TGF-beta. *J. Immunol* 183: 2232–2241. [PubMed: 19635906]

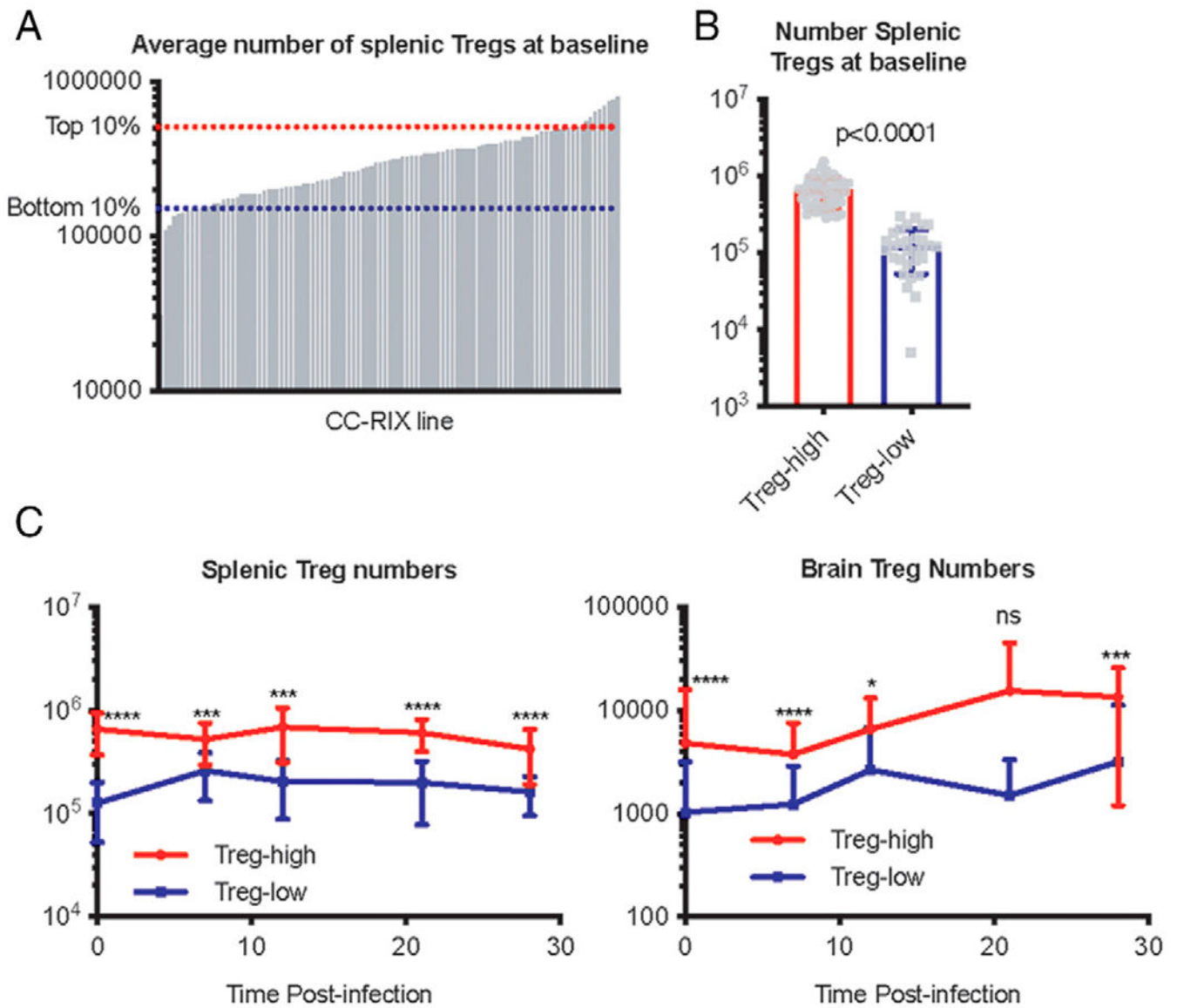


FIGURE 1. Genetically diverse mice display a range of frequencies and numbers of Tregs in the spleen and brain at steady state and postinfection.

(A) Average baseline Treg number (Foxp3⁺CD4⁺ T cells) in the spleen are plotted in rank order for each CC-RIX line. Red dotted line indicates lines with the top 10% number of Tregs ($n = 10$ CC-RIX lines), and blue dotted line indicates lines with the bottom 10% number of Tregs ($n = 10$ CC-RIX lines). (B) Number of splenic Tregs at baseline in CC-RIX lines with the top 10 (red) and bottom 10 (blue) average number of splenic Tregs. Cohorts of age-matched CC-RIX male mice were infected with 100 PFU WNV. At the indicated times postinfection, cohorts of 3–6 mice were euthanized, and the number of CD4⁺Foxp3⁺ Tregs in the spleen or brain was determined by flow cytometry (C). The indicated p values were determined using unpaired t test. The p values from 0.01 to 0.05 are significant (*), $p = 0.001$ to 0.01 are very significant (**), and both $p = 0.001$ to 0.0001 (***) and $p < 0.0001$ (****) are extremely significant.

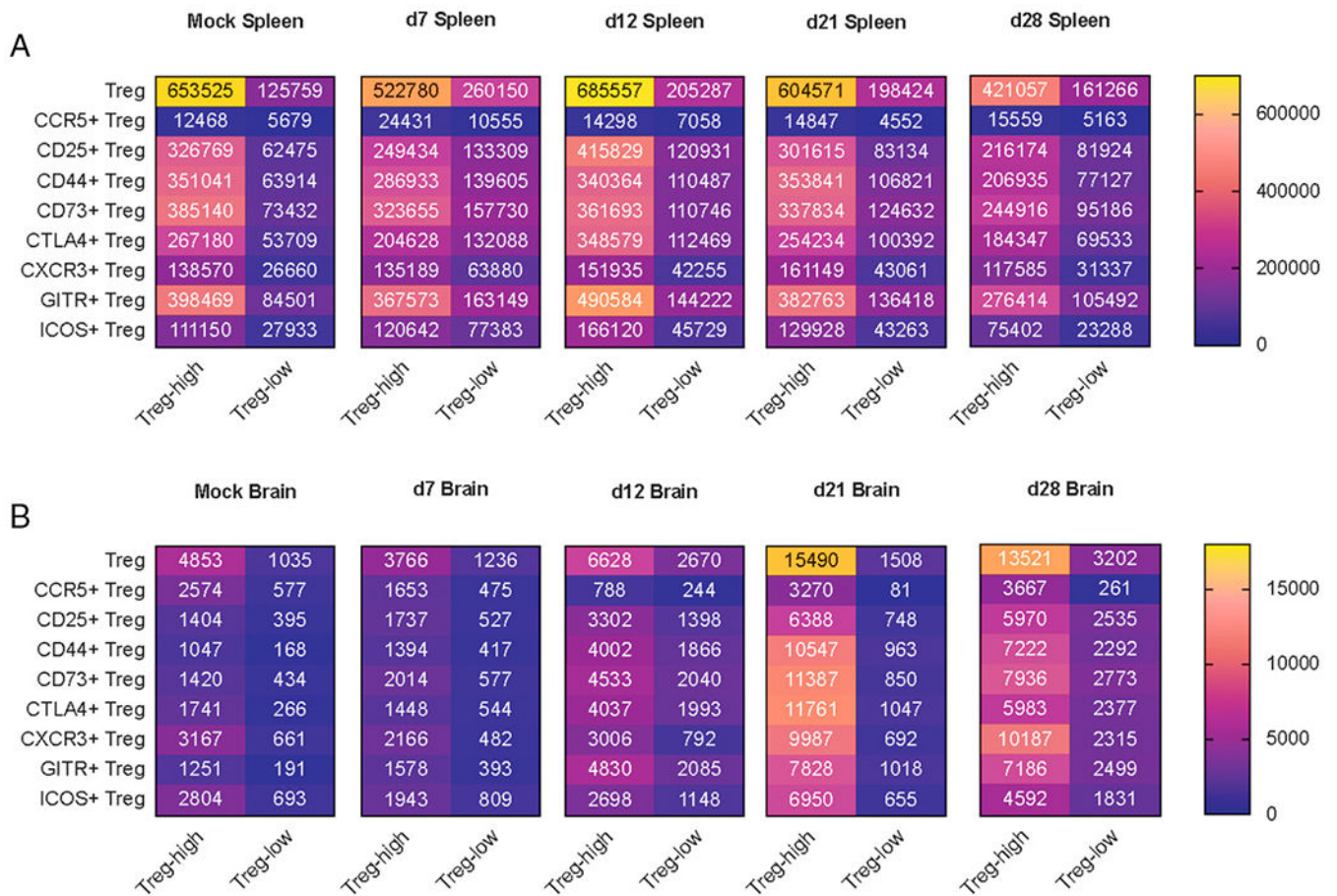


FIGURE 2. Higher Treg numbers at baseline correlate with an activated Treg phenotype postinfection in the spleen and brain.

Cohorts of age-matched CC-RIX male mice were infected with 100 PFU WNV. At the indicated times postinfection, cohorts of 3–6 mice were euthanized, and the number of CD4⁺Foxp3⁺ Tregs expressing the indicated activation markers in the spleen (A) or brain (B) was determined by flow cytometry. Numbers in the heat map cells represent the mean number of the indicated cell type in CC-RIX lines with the top 10 baseline average number of splenic or brain Tregs (Top 10%) or the bottom 10 baseline average number of splenic Tregs (Bottom 10%).

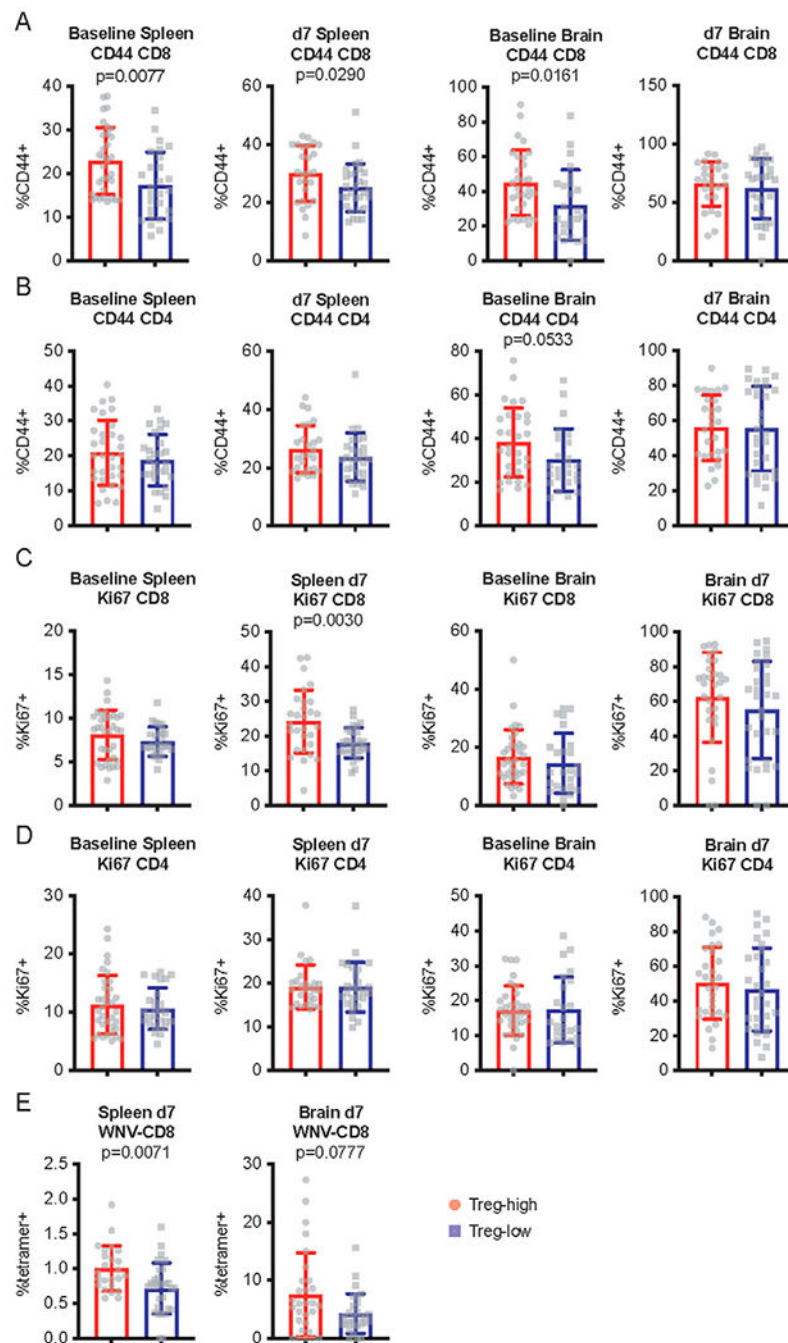


FIGURE 3. Baseline Treg numbers predict the T cell phenotype in lymphoid and peripheral tissues at steady state and following WNV infection.

Cohorts of age-matched CC-RIX male mice were infected with 100 PFU WNV. At the indicated times postinfection, cohorts of 3–6 mice were euthanized, and the frequency of CD4⁺ or CD8⁺ T cells expressing the indicated phenotypic markers in the spleen was determined by flow cytometry. Mice in Treg-high groups are from CC-RIX lines with baseline splenic Treg numbers in the top 10% (red), and mice in the Treg-low groups are from CC-RIX lines with baseline splenic Treg numbers in the bottom 10% (blue). (A)

Frequency of splenic or brain CD8 T cells expressing CD44 either at baseline (mock infected) or at d7 postinfection. **(B)** Frequency of splenic or brain CD4 T cells expressing CD44 either at baseline or at d7 postinfection. **(C)** Frequency of splenic or brain CD8 T cells expressing Ki67 at baseline or d7 postinfection. **(D)** Frequency of splenic or brain CD4 T cells expressing Ki67 at baseline or d7 postinfection. **(E)** Frequency of splenic or brain CD8 cells that are WNV NS4b tetramer⁺ at d7 postinfection. The indicated *p* values were determined using the Mann–Whitney test.

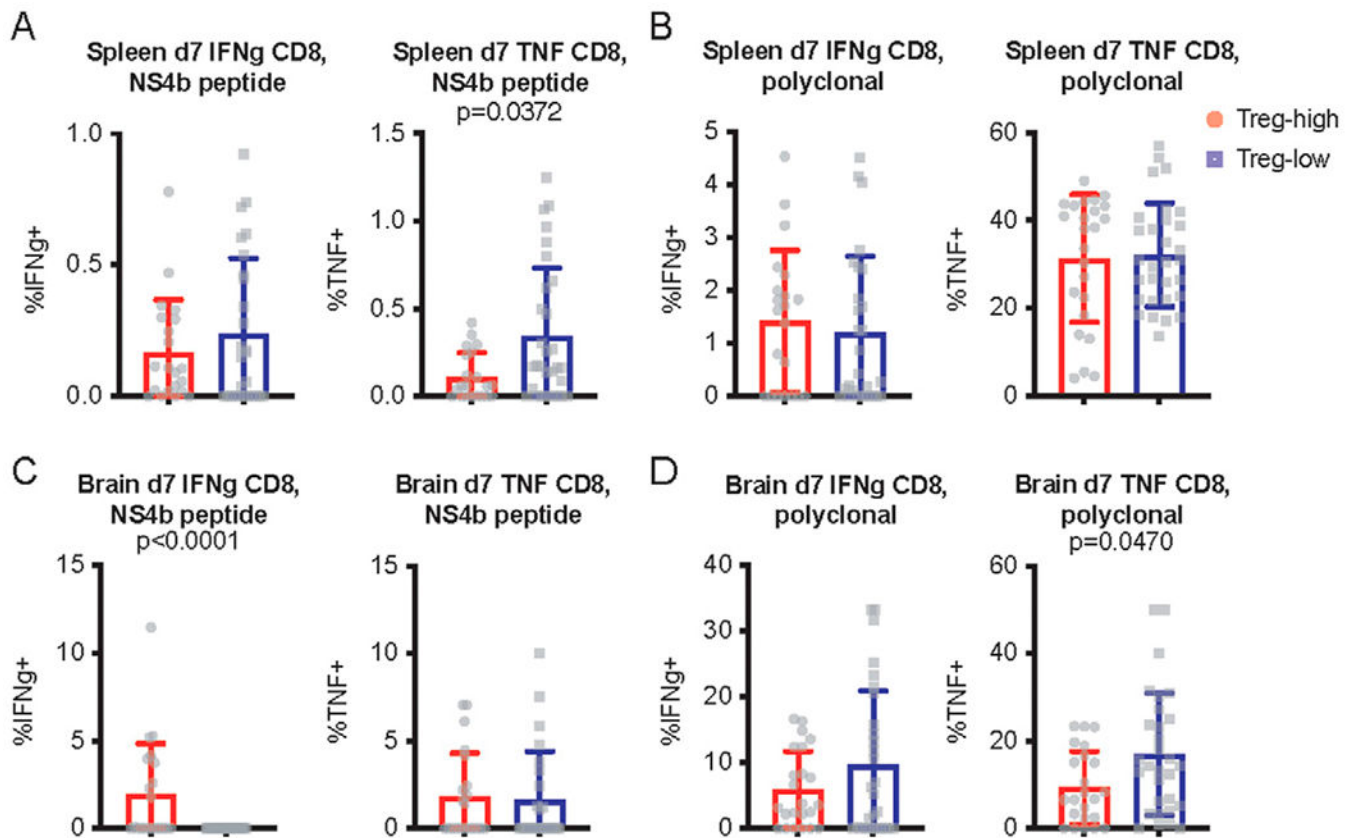


FIGURE 4. Elevated numbers of Tregs at baseline associated with reduced capacity of CD8 T cells to express TNF postinfection.

Cohorts of age-matched CC-RIX male mice were infected with 100 PFU WNV. At the indicated times postinfection, cohorts of 3–6 mice were euthanized, and single cell suspensions from the indicated tissue was stimulated ex vivo with WNV NS4b peptide (A) or anti-CD3/CD28 (B) for intracellular cytokine staining assessment of the frequency of CD8⁺ T cells expressing the indicated cytokines in the spleen (A and B) or brain (C and D). Mice in Treg-high groups are from CC-RIX lines with baseline splenic Treg numbers in the top 10% (red), and mice in the Treg-low groups are from CC-RIX lines with baseline splenic Treg numbers in the bottom 10% (blue). The indicated p values were determined using the Mann–Whitney test. Outliers were identified by ROUT ($Q = 1\%$).

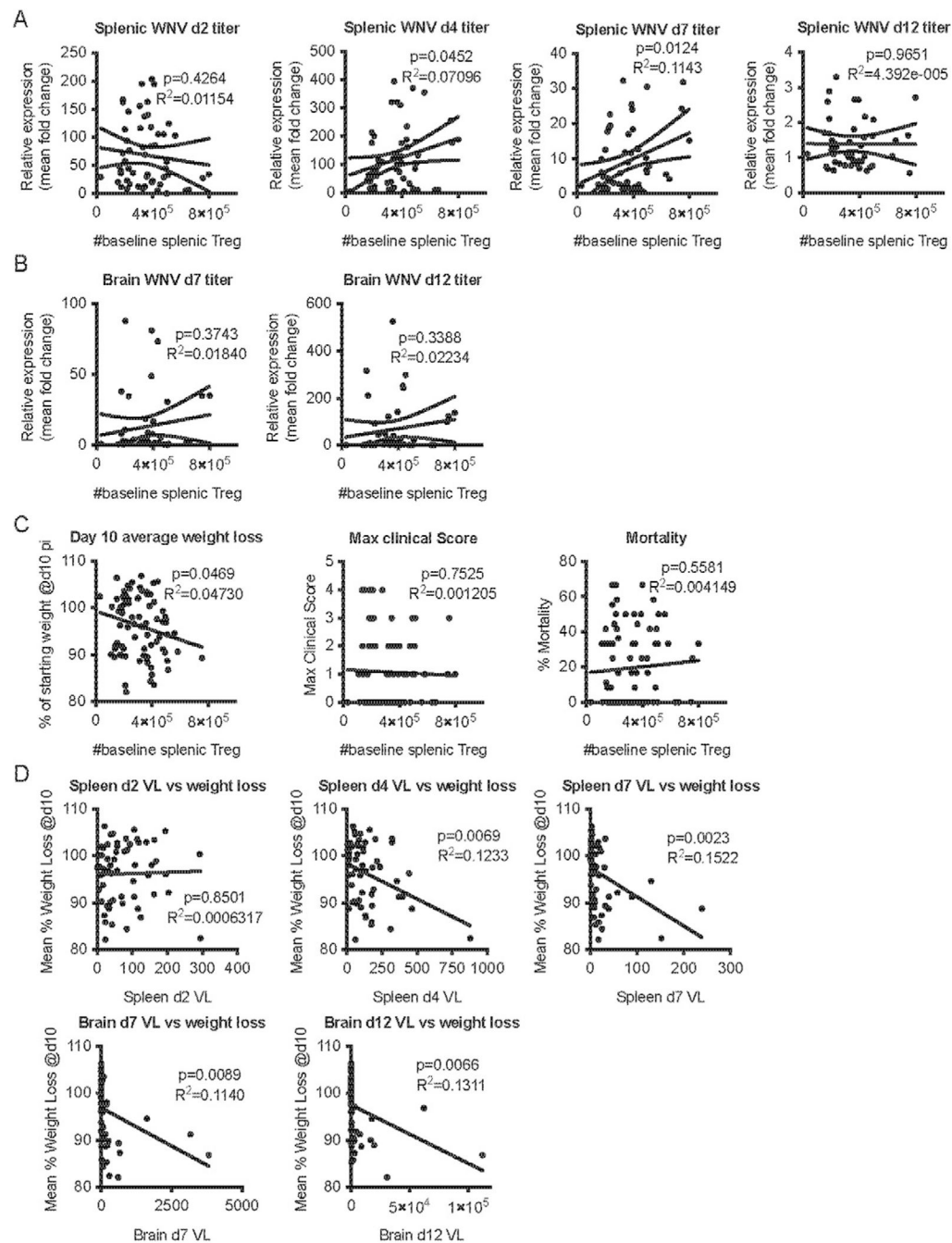


FIGURE 5. Baseline Treg numbers predict high VL following WNV infection.

Cohorts of age-matched CC-RIX male mice were infected with 100 PFU WNV. (A and B) At the indicated times postinfection, age-matched male mice were euthanized, and spleens and brains were harvested and prepared for quantitative RT-PCR to quantify WNV load. A second cohort of age-matched, uninfected CC-RIX male mice were euthanized, and the number of Foxp3⁺ Tregs in the spleen was determined by flow cytometry. Linear regression was performed using the mean number of splenic Tregs at baseline and the mean WNV VL in the indicated tissue and time postinfection. (C) Mortality, clinical score, and average

weight loss at d10 postinfection were monitored continuously following infection, and linear regression was performed using this data in combination with the number of splenic Tregs at baseline. (D) Spleen VL at d2, day 4, or d7 postinfection or brain VL at d7 or day 12 postinfection are plotted against the average weight loss at d10 postinfection for all CC-RIX lines examined in the screen. Outliers were identified by ROUT (Q = 1%). Linear regression was performed using GraphPad Prism.

Author Manuscript

Author Manuscript

Author Manuscript

Author Manuscript

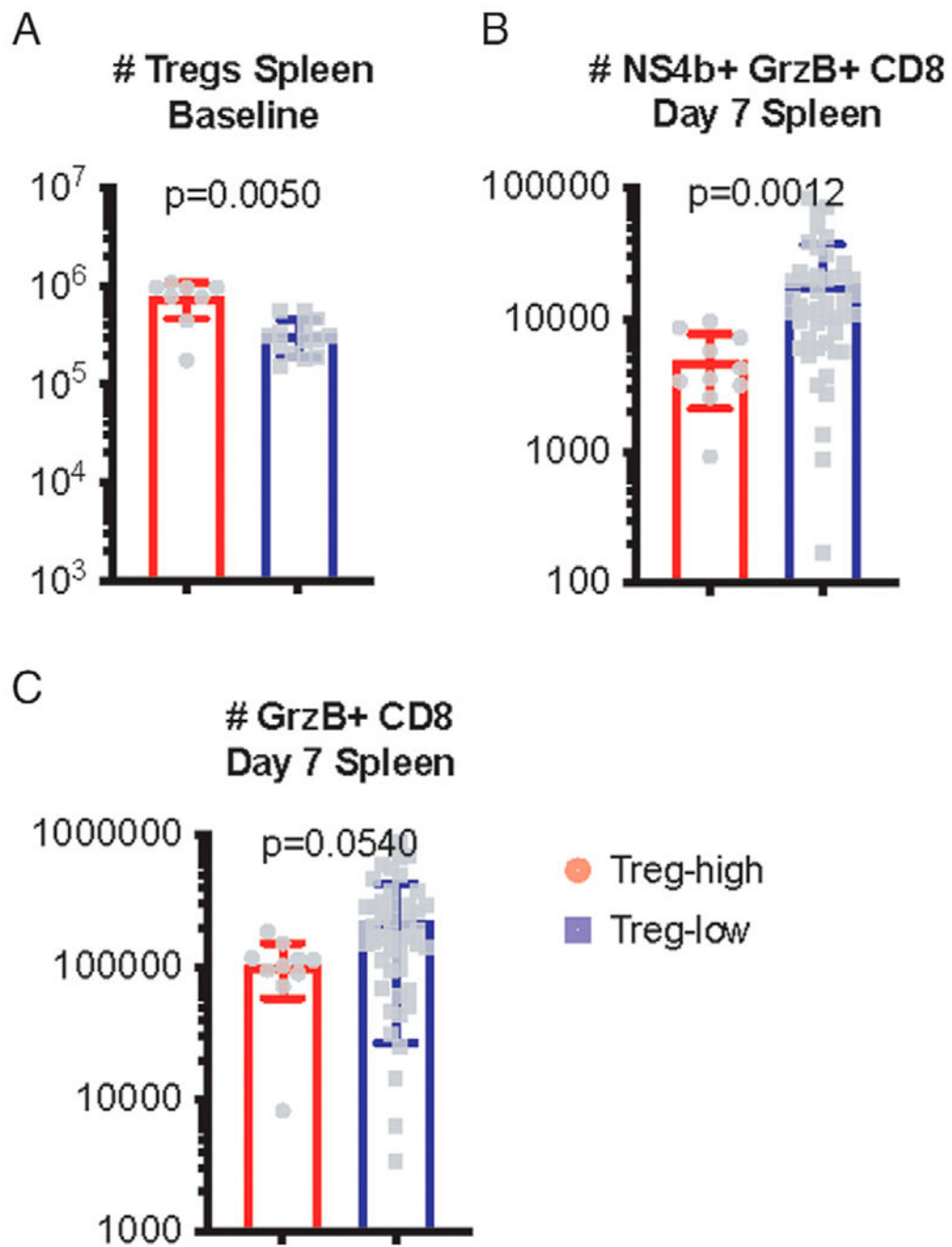


FIGURE 6. Lower baseline number of Tregs is associated with a subsequent cytotoxic phenotype of WNV-specific CD8 T cells upon infection.

A separate validation study of select CC-RIX lines with extreme phenotypes of high or low numbers of Treg at baseline was performed. (A) Age-matched male CC-RIX mice with a high or low number of splenic Tregs at baseline were used to determine (B) the number of granzyme B⁺ NS4b tetramer⁺ CD8 T cells in the spleen at d7 post-WNV infection and (C) the number of granzyme B⁺ CD8 T cells in the spleen at d7 post-WNV infection. The indicated *p* values were determined using the Mann-Whitney test.

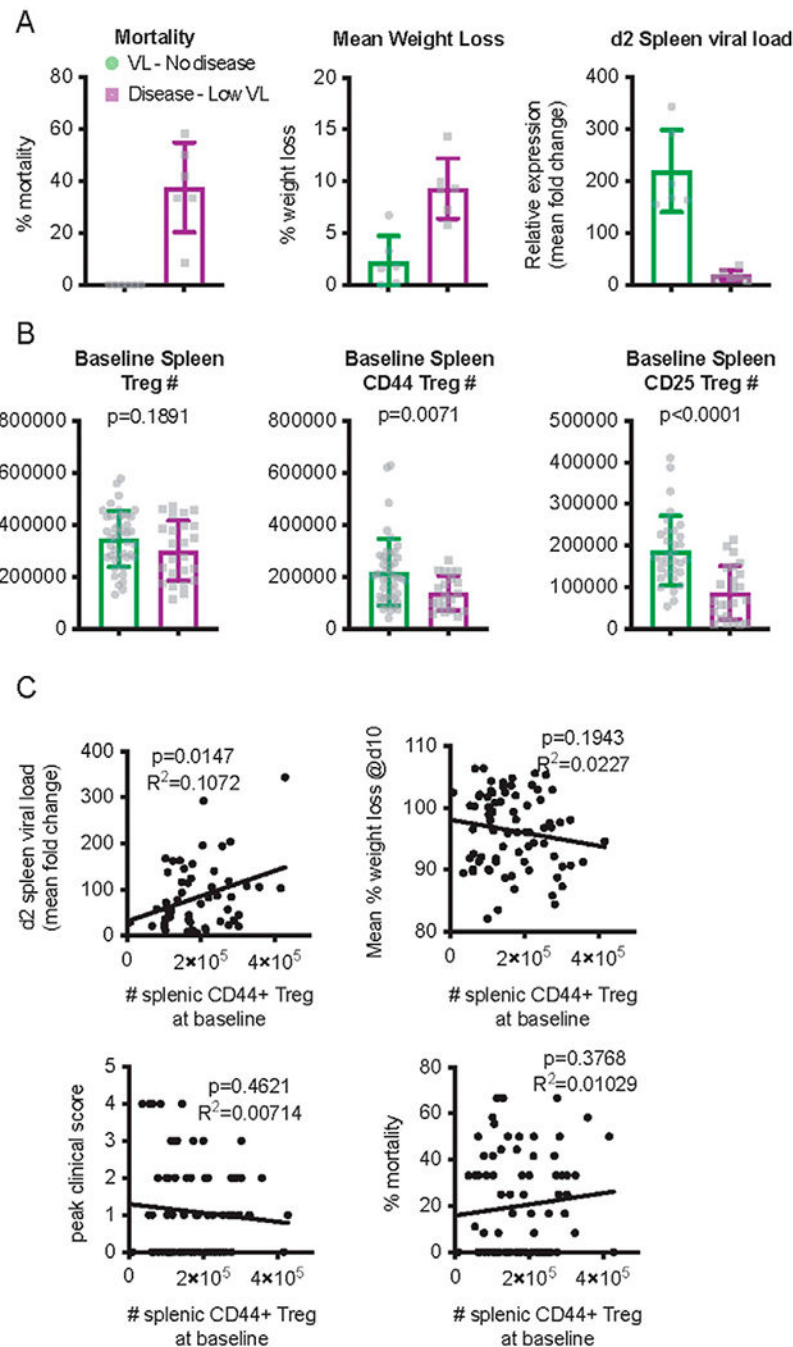


FIGURE 7. Homeostatic Treg abundance contributes to disease tolerance upon infection with WNV.

Cohorts of age-matched CC-RIX male mice ($n = 103$) were infected with 100 PFU WNV. CC-RIX lines with extreme phenotypes were selected for further analysis based on splenic VL, mortality, and weight loss postinfection. Lines that had a high splenic VL at d2 postinfection but had little to no evidence of disease throughout the course of infection ($n = 6$) are termed VL-no disease, and lines that had low splenic VL at d2 postinfection (and through to day 12 postinfection) but did have evidence of disease in terms of mortality

and/or mean weight loss >10% ($n = 6$) are termed disease-low VL. **(A)** Mortality, mean weight loss, and spleen VL at d2 postinfection are shown for the two groups, VL-no disease and disease-low VL. **(B)** The number of splenic Tregs, splenic CD44⁺ Treg, or splenic CD25⁺ Treg at baseline are shown for mice in the VL-no disease and disease-low VL groups. The indicated p values were determined using the Mann–Whitney test. **(C)** Outliers were identified by ROUT ($Q = 1\%$). Linear regressions were performed using GraphPad Prism to test the association of the number of splenic CD44⁺ Treg at baseline with the d2 spleen VL, weight loss, peak clinical score, and mortality in all CC-RIX lines tested.

Author Manuscript

Author Manuscript

Author Manuscript

Author Manuscript

TABLE I.

Ab clones used for flow cytometry

Ab	Clone
Foxp3	FJK-16s
CD3e	145-2C11
CD4	RM4-5
CD8	53-6.7
CD25	PC61
CCR5	HM-CCR5
CD44	IM7
CD73	TY/11.8
Ki67	SolA15
CTLA-4	UC10-4B9
CXCR3	CXCR3-173
GITR	DTA-1
ICOS	7E.17G9
IFN- γ	XMG1.2
TNF	MP6-XT22
Live/dead	N/A

Author Manuscript

Author Manuscript

Author Manuscript

Author Manuscript

TABLE II.

CC-RIX lines and Treg baseline categories

CC-RIX Line	Baseline Treg Numbers	Group
CC061 × CC026	508577	Treg-high
CC001 × CC055	514793	Treg-high
CC015 × CC018	559053	Treg-high
CC043 × CC033	583323	Treg-high
CC046 × CC068	634010	Treg-high
CC033 × CC046	657883	Treg-high
CC055 × CC006	694561	Treg-high
CC030 × CC061	745622	Treg-high
CC051 × CC005	755278	Treg-high
CC052 × CC014	799264	Treg-high
CC008 × CC010	30701	Treg-low
CC065 × CC072	108387	Treg-low
CC006 × CC039	115838	Treg-low
CC074 × CC058	134000	Treg-low
CC075 × CC035	137471	Treg-low
CC072 × CC063	140108	Treg-low
CC063 × CC001	142478	Treg-low
CC068 × CC035	148502	Treg-low
CC033 × CC046	149147	Treg-low
CC019 × CC027	150957	Treg-low

Author Manuscript

Author Manuscript

Author Manuscript

Author Manuscript